Soft Matter

PAPER

Trade-off mechanism of honey bee sucking and lapping†

Jiangkun Wei,‡[a] Fabian Brau, ‡[b] Pascal Damman, [c] Ayrton Draux, [c] Hoa-Ai Béatrice Hua,[b] Zhigang Wu*[a] and Jianing Wu *[a]

Animals have developed various drinking strategies in capturing liquid to feed or to stay hydrated. In contrast with most animals, honey bees *Apis mellifera* that capture nectar with their tongue, can deliberately switch between sucking and lapping methods. They preferentially suck diluted nectar whereas they are prone to lap concentrated nectar. *In vivo* observations have shown that bees select the feeding method yielding the highest efficiency at a given sugar concentration. In this combined experimental and theoretical investigation, we propose two physical models for suction and lapping mode of capture that explain the transition between these two feeding strategy. The critical viscosity, μ^*, at which the transition occurs, is derived from these models, and agrees well with *in vivo* measurements. The trade-off mechanism of honey bee sucking and lapping may further inspire microfluidics devices with higher capability of transporting liquids across a large range of viscosities.

Introduction

The understanding of the relationship between flowers and pollinators is a long-standing and fascinating topic in ecology and evolutionary biology.[1] Approximately 78% of plant species are pollinated by animals in temperate regions. These animals are largely dominated by insects, especially honey bees (*Apis mellifera*).[2] They normally forage nectar by inserting their proboscises into the floral corolla (Fig. 1A and B). During this process, bees involuntarily spread pollen among flowers offering pollination services to plants.[3] Some correlations between flower morphology and bees' tongue shape are rather intuitive. For example, ecologists have found close size matching between floral nectar tube depth and the bees' proboscis length, indicating their mouthparts have been shaped by coevolution processes with the plants they pollinate.[4]

In contrast, the relation between the nectar sugar concentration and the bees' tongue morphology is more subtle. Even if flowers should *a priori* produce the sweetest possible nectar to attract bees interested by maximizing their energy intake, *in vivo* measurements show that very sweet nectar is not the best for bees. Indeed, there is an optimal sugar concentration for the energy intake.[5] As the sugar concentration of nectar increases, its viscosity grows exponentially making concentrated nectars very difficult to capture.[6,7] To overcome this problem, some honey bees have developed several methods to capture a very wide spectrum of nectars, including highly concentrated ones, while most animals use one specific drinking strategy.[8] With their specific tongue morphology (Fig. 1C and D),[9] they are able to ingest very sweet nectars, and even solid sugar with the help of saliva to dissolve it.[10] In addition to the common lapping method, honey bees are also able to suck less viscous liquids directly through their proboscis composed of a pair of galeae and labial palpi that form a tube that encompass the hairy tongue.[11] However, the reason for switching from sucking to lapping method remains unknown. The purpose of this combined experimental and theoretical study is to rationalize the observed transition between the two feeding methods using physical models. This study may inspire ultimately the design of highly-efficient microfluidic devices capable of transporting fluids with viscosities across three orders of magnitude.

Results and discussion

Switchable feeding methods of sucking and lapping

To characterize the sucking and lapping modes, we fed honey bees with blue-dyed sucrose solutions of contrasted viscosities (20% and 50% wt/wt) contained in a capillary tube of inner diameter $D_c = 1$ mm, much larger than the width of tongue to

[a] *School of Aeronautics and Astronautics, Sun Yat-Sen University, Guangzhou, 510006, People's Republic of China. E-mail: wuzhigang@mail.sysu.edu.cn, wujn27@mail.sysu.edu.cn*

[b] *Université libre de Bruxelles (ULB), Nonlinear Physical Chemistry Unit, CP231, 1050, Brussels, Belgium*

[c] *Université de Mons (UMons), Laboratoire InFlux, 7000, Mons, Belgium*

† Electronic supplementary information (ESI) available: Including an appendix and Video S1 can be found online. See DOI: https://doi.org/10.1039/d2sm00361a
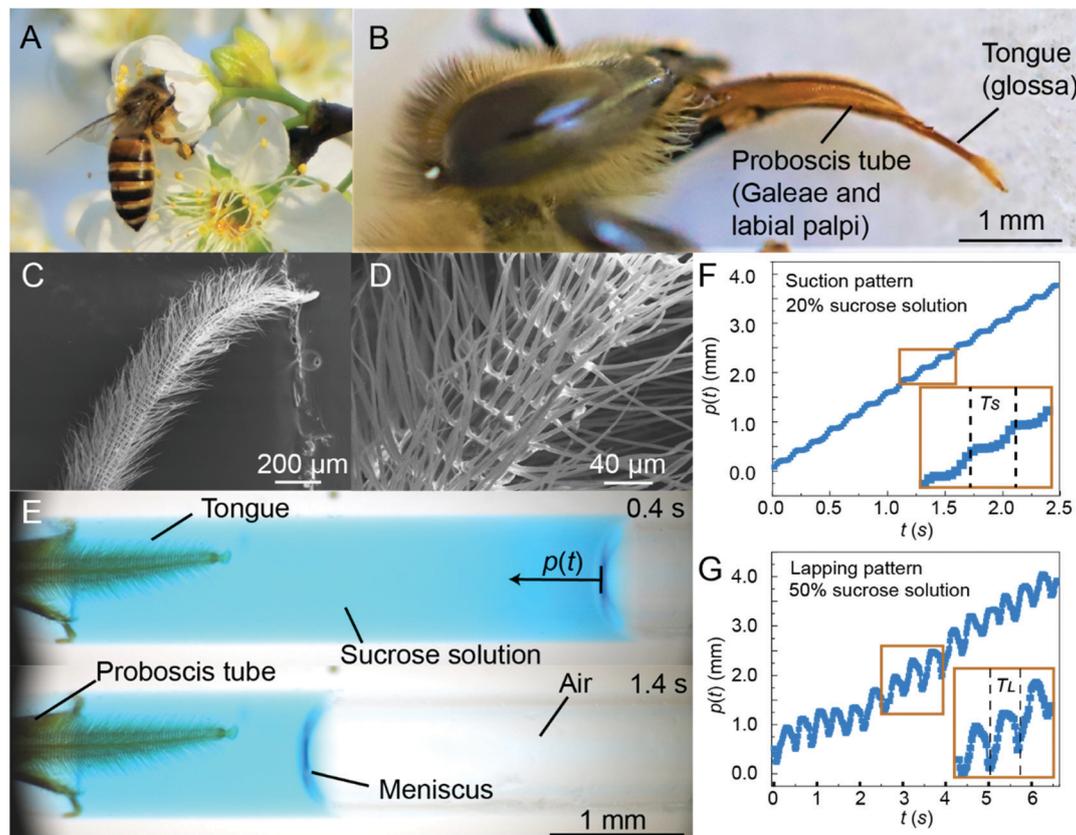‡ These authors contributed equally to the work.

Fig. 1 Honey bee sucking and lapping feeding methods. (A) Honey bee foraging nectar inside a flower. (B) Image showing a lateral view of a honey bee head. The main feeding apparatus is composed of a proboscis tube (galeae and labial palpi) that encompasses a hairy tongue (glossa). (C) and (D) SEM images showing the dense hairs attached on the segmental rings of the tongue. (E) Two video frames showing a honey bee sucking nectar (20%) in a capillary tube where the tongue is still and protracted and its hairs erected. (F) and (G) Variation of the position $p(t)$ of the liquid meniscus as a function of time during the suction and lapping process. T_S and T_L denote one typical cycle of head pump sucking and one typical cycle of tongue lapping, respectively.

limit hydrodynamic wall effects (Fig. 1E and Video S1, ESI†). The position $p(t)$ of the meniscus at the liquid–air interface was measured as a function of time, and the ingestion rate was obtained from $Q(t) = \pi D_c^2 v_m(t)/4$, where $v_m(t) = dp(t)/dt$ is the velocity of the meniscus. Since, in average $p(t) \sim t$, v_m and Q remain essentially constant (Fig. 1F and G). For the low viscosity solution (20% wt/wt), the bee sucks the nectar. In this case, the temporal variation of the meniscus position $p(t)$ reveals a staircase curve with extremely regular and continuous increases related to the periodic operation of the sucking pump located in the bee's head (Fig. 1F). For the high viscosity solution (50% wt/wt), the bee laps the nectar. Now, the meniscus position exhibits regular back-and-forth motion superimposed to a continuous linear increase (Fig. 1G). These periodic variations are related to the fact that, when the honey bee protracts its tongue to lap the nectar, the liquid meniscus recedes due to the immersion volume of the tongue. This phenomenon is not observed in the suction mode since the tongue stays immersed in the liquid during its capture. The sucking and lapping frequency are both found to be about 4–6 Hz. The feeding rates inferred from the meniscus position for various sugar concentrations are shown in Fig. 5.[11]

A detailed analysis of the lapping mechanism has been previously described in ref. 9 and is briefly recalled here below. We now focus on the sucking mode of fluid capture.

Sucking mechanism

According to previous studies,[12] the cibarial pump inside bee's head creates a pressure gradient along the proboscis, which is responsible for nectar uptake. (Fig. 2A). To measure the flow velocity inside the capillary tube while the bee is sucking the fluid, we perform a PIV analysis. For this purpose, we record videos of the feeding process for low viscosity sucrose solution (20%) mixed with microparticles (5 μm Polyamid seeding particles, Dantec Dynamics, Denmark) (Fig. 2B). The PIV analysis confirms the periodic fluctuations of the fluid velocity around an average value $\bar{u} \simeq 1.5$ mm s^{-1}. Considering the viscosity μ and the density ρ of the sucrose solution (10–50%),[9] the Reynolds number Re $= 2\rho\bar{u}R_c/\mu < 1$, where $R_c \sim 0.2$ mm is the radius of the proboscis tube (Fig. 2E), indicating that the inertial effects can be neglected. The Womersley number, Wo $= h_p\sqrt{2\pi f\rho/\mu} < 1$, where h_p is the pump maximum
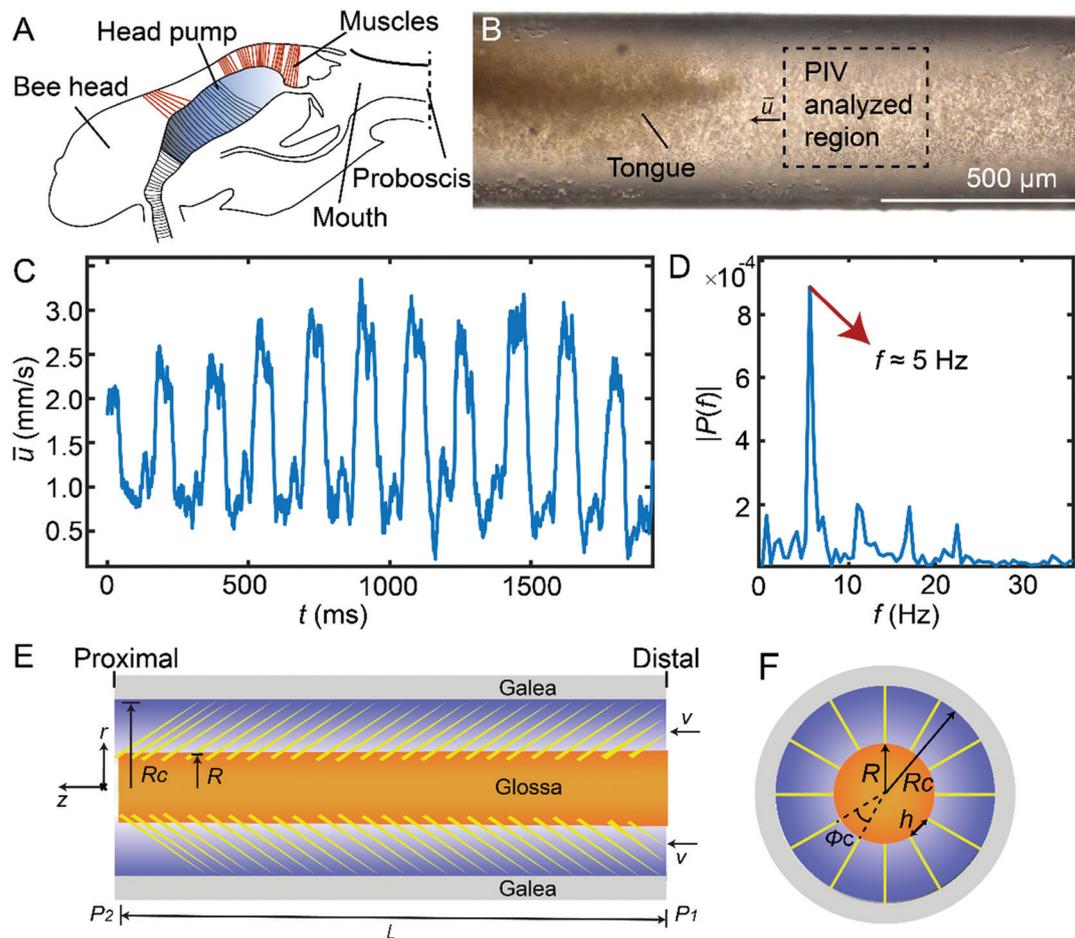
Fig. 2 Honey bee sucking mechanism. (A) Schematic showing the sucking pump inside the head. The suction pressure difference is generated by the action of the pump muscles. (B) Honey bee sucking in a capillary tube filled with sucrose solution (20%) mixed with microparticles. The rectangular dashed line region is the PIV analysis area. Average velocity along the tube axis in the rectangular region is denoted by $\bar{u}$ and its time variation is presented in (C). (D) Single-sided amplitude spectrum of $\bar{u}$ derived by Fast Fourier transform analysis. The peak value representing the suction frequency of the honey bee. Schematic view of the suction proboscis tube as used in the model: (E) longitudinal view; (F) cross-section view.

diameter that cannot exceed the head size (~ 0.1 mm), indicates that the unsteady effects of flow can be also neglected.[12]

To derive a physical model of the honey bee sucking process, we consider the flow inside a micro-structured device made of hairs of length L_h and radius R_h attached to a cylindrical tongue of length L and radius R and bounded by a cylindrical tube of radius R_c mimicking the galea (Fig. 2E). We use cylindrical coordinates, and assume that there is no flow along the radial and azimuthal directions, $v_r = v_\phi = 0$, in agreement with PIV measurements. Mass conservation imposes that

$$\nabla \cdot \boldsymbol{v} = \frac{1}{r}\frac{\partial}{\partial r}(rv_r) + \frac{1}{r}\frac{\partial v_\phi}{\partial \phi} + \frac{\partial v_z}{\partial z} = \frac{\partial v_z}{\partial z} = 0 \tag{1}$$

$$\Rightarrow \boldsymbol{v} = v_z(r,\phi)\boldsymbol{e}_z$$

Therefore, the flow is only along the z-direction and does not vary along z. In addition, because the flow is unidirectional, the Navier–Stokes equation becomes linear since the nonlinear convection term vanishes identically: $(\boldsymbol{v}\cdot\nabla)\boldsymbol{v} = v_z(\partial v_z/\partial z)\boldsymbol{e}_z = 0$.

Then, after neglecting the gravitational term, the Navier–Stokes equation simplifies to

$$\rho\frac{\partial v_z}{\partial t} = -\frac{\partial P}{\partial z} + \mu\nabla^2 v_z \tag{2}$$

Because v_z is independent of z, taking the z-derivative of eqn (2) leads to $\partial P/\partial z =$ const. $= -\Delta P/L$, where $\Delta P = P_1 - P_2 > 0$ and P_1, P_2 are the pressures at the two extremities of the system, see Fig. 2E. We now search for a stationary solution, *i.e.* $\partial_t v_z = 0$, so eqn (2) becomes

$$\frac{\partial^2 v_z}{\partial r^2} + \frac{1}{r}\frac{\partial v_z}{\partial r} + \frac{1}{r^2}\frac{\partial^2 v_z}{\partial \phi^2} + \frac{\Delta P}{\mu L} = 0 \tag{3}$$

where the Laplacian operator has been written explicitly in cylindrical coordinates. Now, we consider the presence of hairs in the system. They are roughly arranged along the glossa according to a hexagonal lattice. However, in the proposed model, we assume that hairs delimit annular sectors of angle ϕ_c bounded by the glossa of radius R and the galea of radius R_c (Fig. 2F). Indeed, it has been shown that the flow inside

hexagonal or square lattices of pillars can be well approximated by the flow within such a channeled structure provided that its dimensions correspond to the lattice mesh size.[13,14] Due to the non-slip boundary condition, the velocity vanishes at the hair walls. Let ϕ_c be the angular distance between two adjacent hairs (see Fig. 2F), we have

$$v_z(r, \phi = 0) = v_z(r, \phi = \phi_c) = 0 \tag{4}$$

An exact solution of eqn (3) with the boundary conditions (4) and non-slip boundary conditions at $r = R$ and R_c is known.[15,16] However, this solution is cumbersome, and we will instead derive a simple approximate expression for the flow rate which agrees well with the exact expression, see Appendix. For this purpose, we use the following ansatz to satisfy the boundary conditions (4), see for instance,[14]

$$v_z(r, \phi) = \bar{v}_z(r)f(\phi) = \bar{v}_z(r)\frac{6\phi(\phi_c - \phi)}{\phi_c^2} \tag{5}$$

Substituting (5) into eqn (3), we have

$$f(\phi)\frac{\partial^2 \bar{v}_z}{\partial r^2} + \frac{f(\phi)\partial \bar{v}_z}{r \ \partial r} + \frac{\bar{v}_z \partial^2 f(\phi)}{r^2 \ \partial \phi^2} + \frac{\Delta P}{\mu L} = 0 \tag{6}$$

We now compute the mean flow along z by taking the average along the ϕ direction. Noting that $\phi_c^{-1}\int_0^{\phi_c} f(\phi)\mathrm{d}\phi = 1$, $\phi_c^{-1}\int_0^{\phi_c}\partial^2 f(\phi)/\partial\phi^2\mathrm{d}\phi = -12/\phi_c^2$, the ϕ-average of eqn (6) reads

$$\frac{\partial^2 \bar{v}_z}{\partial r^2} + \frac{1}{r}\frac{\partial \bar{v}_z}{\partial r} - \frac{12R^2}{h^2}\frac{\bar{v}_z}{r^2} + \frac{\Delta P}{\mu L} = 0 \tag{7}$$

where we have used $\phi_c = h/R$ with h the distance between the base of two adjacent hairs (see Fig. 2F). Eqn (7) is the main equation. Once it is solved, the velocity field is given by $\mathbf{v} = [6\bar{v}_z(r)\phi(\phi_c - \phi)/\phi_c^2]\mathbf{e}_z$. This is the velocity in the angular section $0 \leq \phi \leq \phi_c$. There are $N = 2\pi/\phi_c$ of such a sector. To solve eqn (7), we need to specify two boundary conditions for $\bar{v}_z$. Let R be the glossa radius and $R_c > R$ be the radial position of the galea, see Fig. 2E. We consider the flow taking place in the region $R \leq r \leq R_c$ which is filled by hairs. Therefore, we need to solve eqn (7) with the boundary conditions

$$\bar{v}_z(r = R) = \bar{v}_z(r = R_c) = 0. \tag{8}$$

The solution of eqn (7) with the boundary conditions (8) reads

$$\bar{v}_z(r) = \frac{R^2\Delta P}{\mu L}g(\bar{r}, \bar{k}, \bar{R}_c), \quad g = c_1\bar{r}^k + c_2\bar{r}^{-k} + \frac{\bar{r}^2}{k^2 - 4} \tag{9}$$

where $c_1 = (1 - \bar{R}_c^{2+k})/[(k^2 - 4)(\bar{R}_c^{2k} - 1)]$, $c_2 = (\bar{R}_c^{2+k} - \bar{R}_c^{2k})/[(k^2 - 4)(\bar{R}_c^{2k} - 1)]$, $\bar{r} = r/R$, $\bar{R}_c = R_c/R$ and $k = \sqrt{12}R/h = \sqrt{12}/\phi_c \sim N$. Notice that this solution is valid provided $k \neq 2$. The solution can also be computed analytically when $k = 2$. However, in our case, $h < R$ so that $k > 2$. We can now compute the flow rate $Q_S = N\int_R^{R_c} r\mathrm{d}r\int_0^{\phi_c}\bar{v}_z(r)f(\phi)\mathrm{d}\phi$, where $N = 2\pi/\phi_c$ is the number of angular sectors and $f(\phi)$ is defined by eqn (5). Computing the integral over ϕ, we get $Q_S = 2\pi\int_R^{R_c} r\bar{v}_z(r)\mathrm{d}r = (2\pi R^4\Delta P/\mu L)\int_1^{\bar{R}_c}\bar{r}g(\bar{r}, k, \bar{R}_c)\mathrm{d}\bar{r}$, where we

used eqn (9) and the change of variable $\bar{r} = r/R$. The remaining integral can be computed exactly and we get

$$Q_S = \frac{2\pi R^4\Delta P}{\mu L}F(k, \bar{R}_c) \tag{10}$$

where

$$\begin{aligned} F = &\left\{(k-2)^2\left(\bar{R}_c^{2k+4} + 1\right) - (k+2)^2\left(\bar{R}_c^{2k} + \bar{R}_c^4\right)\right. \\ &\left. + 16k\bar{R}_c^{k+2}\right\}\left[4\left(k^2 - 4\right)^2\left(\bar{R}_c^{2k} - 1\right)\right]^{-1}. \end{aligned} \tag{11}$$

The function F looks complicated but has simple asymptotic behaviors

$$\begin{cases} F \simeq \dfrac{(\bar{R}_c - 1)^3}{12} & \text{for} \quad \bar{R}_c \simeq 1, \\ F \simeq \dfrac{\bar{R}_c^4}{16} & \text{for} \quad k \ll 1, \bar{R}_c \gg 1, \\ F \simeq \dfrac{\bar{R}_c^4 - 1}{4k^2} & \text{for} \quad k \gg 1, \bar{R}_c \geq 2. \end{cases} \tag{12}$$

Eqn (12) shows how the flow rate behaves in a very narrow gap, i.e. $R \simeq R_c$. Note also that in the limit of a large gap, $\bar{R}_c \gg 1$, and a low hair density, $k \ll 1$, we recover as expected the standard expression of a Poiseuille flow in a tube of radius R_c, i.e. $Q_S = \pi R_c^4\Delta P/(8\mu L)$. The variation of the function F, defined by eqn (11), as a function of $\bar{R}_c$ is shown in Fig. 3A and B for several values of k together with the asymptotic behaviors (12).

The relevant regime for honey bees is the last one given by eqn (12), so that the flow rate given by eqn (10) simplifies to

$$Q_S = \frac{\pi}{24}\frac{\Delta P\left(R_c^4 - R^4\right)h^2}{\mu L}\frac{1}{R^2}. \tag{13}$$

This relation shows obviously that Q vanishes when R_c tends to R or h tends to 0. This is a Poiseuille-like expression where the geometric factor $h/R \ll 1$ takes into account the presence of hairs which impacts the flow rate.

Since there is no reported study about honey bees, we estimate the pressure difference, ΔP, generated by the head pump from data reported for butterflies. By measuring the dependence of flow rate on sugar concentration, Pivnick and McNeil inferred that butterflies apply an essentially constant suction power $\dot{W}$ in drinking, regardless of the sugar concentration of the nectar.[17] Indeed, Fig. 5 of ref. 17 suggests that

$$2.2 \times 10^{-7}\ \text{J s}^{-1} \leq \dot{W} \leq 4.6 \times 10^{-7}\ \text{J s}^{-1} \tag{14}$$

at $T = 25\ ^\circ\text{C}$ when the sugar concentration varies from 10 to 65%, i.e. when viscosity varies by two orders of magnitude, $10^{-3}\ \text{Pa s} \leq \mu \leq 10^{-1}\ \text{Pa s}$. If we assume that $\dot{W}$ is also essentially constant for bees, we obtain the expression of ΔP in terms of $\dot{W}$
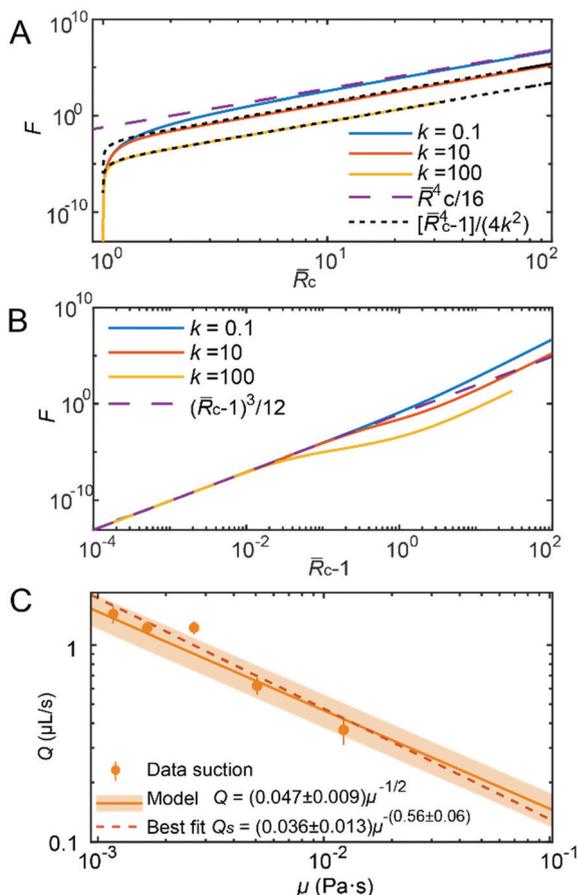
$$\Delta P = \frac{\dot{W}}{Q_S}. \tag{15}$$

Fig. 3 Analysis of honey bee suction. (A) and (B) Variation of the function F defined by eqn (11) as a function of $\bar{R}_c$ for several values of k together with the asymptotic behaviors given by eqn (12). (C) Variation of the ingestion rate Q as a function of the viscosity μ. The data come from ref. 11 eqn (17) and the best power-law fit are also shown.

Substituting this last relation into eqn (13), we obtain

$$Q_S = \left[\frac{\pi \dot{W} \left(R_c^4 - R^4\right)}{24 \quad \mu L}\right]^{\frac{1}{2}} \frac{h}{R}. \qquad (16)$$

Therefore, we get $Q_S \sim \mu^{-\frac{1}{2}}$ and $\Delta P \sim \mu^{\frac{1}{2}}$ in agreement with the models proposed in ref. 7 and 8. This means that bees increase the difference of pressure while feeding on higher-viscosity nectar.

Fig. 3C shows the comparison between eqn (16) and data previously reported in Fig. 2C of ref. 11 plotted as a function of the viscosity instead of sugar concentration (Appendix). It should be noted that no fitting parameters are required once the physiological parameters are experimentally determined. We use the following values: $L = 3$ mm, $R = 70$ μm, $L_h = 180$ μm, $h = 20$ μm, and $R_c = R + L_h \sin(5\pi/18) = 208$ μm, where $5\pi/18$ is the maximum erection angle of tongue hair. For the suction power $\dot{W}$ in eqn (16), we simply use the range of values reported for butterfly, see eqn (14), since the bee has a similar size.[17]

Therefore, we obtain.

$$Q_S = (0.047 \pm 0.009)\mu^{-\frac{1}{2}}, \qquad (17)$$

where μ is measured in Pa s and Q_S in μL s^{-1}. Fig. 3C shows that eqn (17) describes very well the data with an exponent compatible with the one obtained from a power-law fit, namely -0.56 ± 0.06, supporting the proposed model for suction.

Lapping mechanism

The honey bee's lapping method has been examined in detail before[9,18] and we here simply recall the tongue dynamics over one lapping cycle. Honey bee tongue is initially stored inside the proboscis tube and then suddenly protracts out (Fig. 4A and B). As the tongue tip almost reaches the maximum extension position, the hairs that are initially adhering to the tongue begin to unfold to capture the nectar. Finally, the tongue
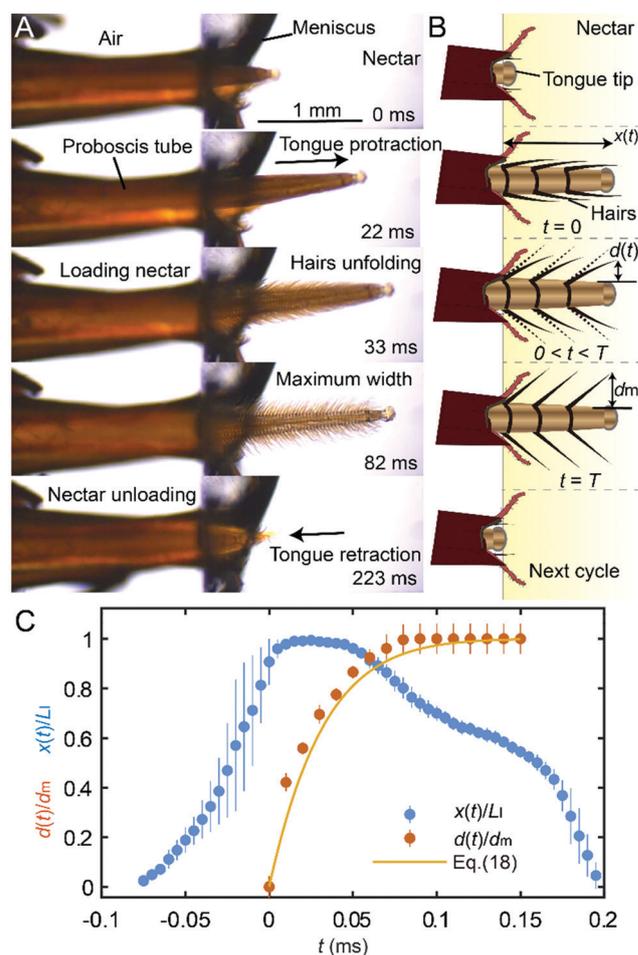

Fig. 4 Lapping cycle of honey bee using the tongue. (A) Time sequence images of a honey bee's typical lapping cycle. (B) Schematic of tongue hairs relaxation dynamics showing the distance d(t) between the hair tip and the glossa and the immersed tongue length, x(t). (C) Variation of the rescaled tongue protraction distances x(t)/L_I and tongue width d(t)/d_m as a function of time t for c = 30%. L_I = 1.6 mm is the maximum immersed length of the tongue, and $d_m = L_h \sin(5\pi/18) \simeq 138$ μm is the maximum expansion width of the hairs, see panel B. Eqn (18) is represented by the yellow curve.

retracts to the proboscis and the nectar is unloaded into the mouth. Since the hairs are very thin, they are bent before to relax to a straight shape during the unfolding process (Fig. 4B). The temporal variation of the distance d(t) between the tip of the hair and the glossa can be estimated by[7]

$$\frac{\mathrm{d}(t)}{d_{\mathrm{m}}} = 1 - \left[1 - \frac{t}{T}\right]^{11}, \quad T = 4.35\left[\frac{\mu^{10}d_{\mathrm{m}}}{\bar{E}^{10}v_{\mathrm{c}}}\right]^{\frac{1}{11}}, \quad (18)$$

where $\bar{E} = ER_{\mathrm{h}}^4/L_{\mathrm{h}}^4$ is an effective hair stiffness, E is the elastic modulus, $d_{\mathrm{m}} = L_{\mathrm{h}}\sin(5\pi/18) \simeq 138\,\mu\mathrm{m}$ the maximum value of d, and $v_{\mathrm{c}} = 4\mu/\rho R_{\mathrm{h}}$ is a characteristic velocity of the fluid flow near the hair. Eqn (18) describes the relaxation dynamics of the tongue hairs as shown schematically in Fig. 4B. At $t = 0$, $d(0) = 0$, and the hairs adhere to the tongue; at $t = T$, $d(T) = d_m$, and the hairs are fully open. As shown in Fig. 4C and eqn (18) is in good quantitative agreement with *in vivo* measurements of the hair relaxation dynamics.

Using eqn (18), we can describe the data reported in ref. 11 for lapping. Again, there are no fitting parameters. The physiological parameters are fixed to $L_{\mathrm{I}} = 1.6$ mm, $R_{\mathrm{h}} = 2.5\,\mu\mathrm{m}$, $T_{\mathrm{L}} = 0.20$ s, $E = 1.1$ MPa, and the same values of R and L_{h} than the ones used with the suction model. The immersion length L_{I} and the lapping time T_{L} have been estimated from Fig. 4A. The volume of nectar collected when the tongue retracts out of nectar at $t = T_{\mathrm{R}} \simeq T_{\mathrm{L}}/2$ is the sum of the volume trapped by the hairs and the volume dragged by a bare LLD mechanism,[7] given by

$$Q_{\mathrm{L}} = \pi v_{\mathrm{R}}[[R + d(T_{\mathrm{R}})^2][1 + 1.34\mathrm{Ca}^{2/3}]^2 - R^2], \quad (19)$$

where $\mathrm{Ca} = \mu v_{\mathrm{R}}/\gamma$ is the capillary number, $v_{\mathrm{R}} = L_{\mathrm{I}}/T_{\mathrm{L}}$ is the average retraction velocity, and $\gamma \simeq 0.074$ N m^{-1} is the liquid surface tension that does not vary significantly with the sugar concentration.[19] Fig. 5A shows a nice agreement between theory and *in vivo* measurements for both feeding methods.

Suction/lapping trade-off

Once the ingestion rate is known, the energy intake rate, $\dot{E}$, is computed from $\dot{E}(c_{\mathrm{s}}) = \sigma Q(c_{\mathrm{s}})\rho_{\mathrm{l}}(c_{\mathrm{s}})c_{\mathrm{s}}$, where c_{s}, $\sigma = 15.48$ kJ g^{-1} and ρ_{l} are, respectively, the sugar concentration, the energy content per unit mass of sugar,[20] and the mass density of nectar which varies with the sugar concentration (Appendix). As for Q, Fig. 5B obviously shows a good agreement between theory and experiments. The maximum of $\dot{E}$ defines the optimal viscosity for each feeding mode which is close to $\mu \sim 0.004$ Pa s (*i.e.*, $c_{\mathrm{s}} = 35\%$ at $T = 30\,^\circ$C) for suction and $\mu \sim 0.011$ Pa s (*i.e.*, $c_{\mathrm{s}} = 49\%$ at $T = 30\,^\circ$C) for lapping.

Fig. 5 shows that the transition between suction and lapping appears around 2–3 mPa s (20–30% wt/wt) in agreement with observations reported in ref. 11 (Fig. 5C). The suction-lapping transition occurs at low sugar concentrations. In this regime, corresponding to the plateau observed at low viscosity in Fig. 5A, the hairs are fully open (d(T_{R}) = d_{m}), and the lapping flow rate simplifies to $Q_{\mathrm{L}} = \pi v_{\mathrm{r}}[R_{\mathrm{c}}^2 - R^2]$. The flow rate for suction Q_{S}, given by eqn (16), is larger than the flow rate for
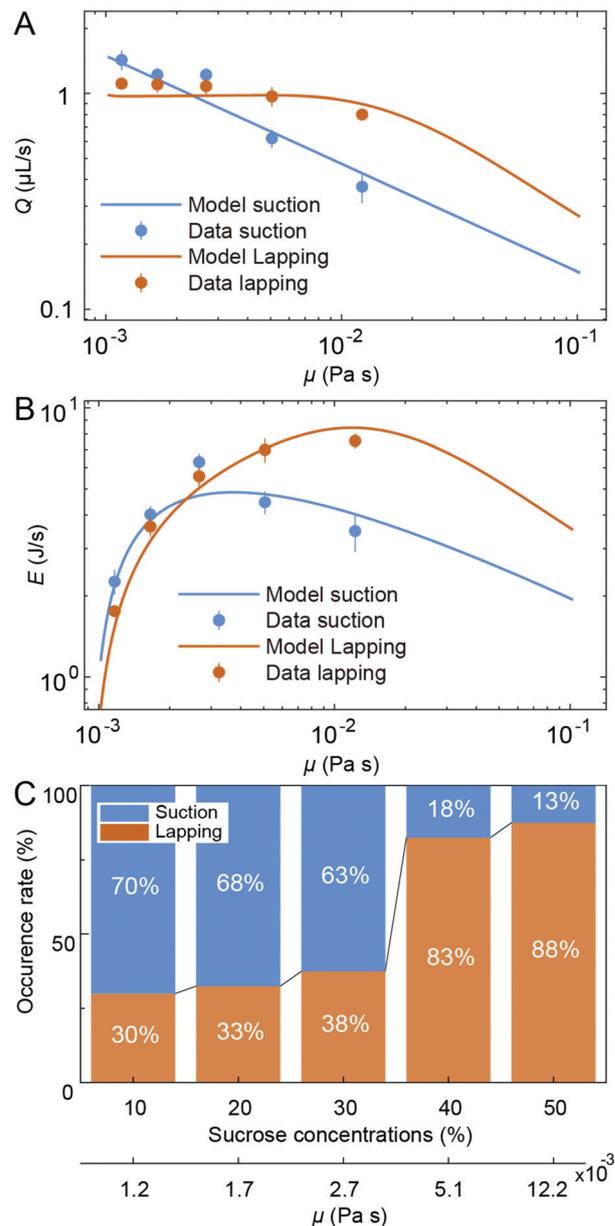

Fig. 5 (A) Comparison between the experimental variation of the ingestion rate Q as a function of the viscosity μ, for the suction and lapping regimes, and eqn (17) for the suction regime and eqn (19) for the lapping regime. The data come from ref. 11. (B) Comparison between the experimental variation of the energy intake rate $\dot{E}$ as a function of the viscosity μ for the suction and lapping regimes together with the corresponding theoretical curves. (C) Occurrence rate of the two feeding modes in honey bees, when feeding on sucrose solutions with various concentrations. The corresponding dynamic viscosity is listed below the sucrose concentration value. The data come from ref. 11.

lapping given above when:

$$\mu < \mu^* = \frac{\dot{W}}{24\pi v_{\mathrm{R}}^2}\frac{(R_{\mathrm{c}}^2 + R^2)}{(R_{\mathrm{c}}^2 - R^2)}\frac{h^2}{LR^2} \quad (20)$$

If we use *Apis* parameters and the average power in eqn (14), we get the viscosity at the transition $\mu^* = 0.0025$ Pa s (*i.e.*, $c_{\mathrm{s}} = 28\%$ at $T = 30\,^\circ$C) which agrees with the data reported in Fig. 5.

Although honey bees (*Apis mellifera*) can switch from sucking to lapping when feeding, we have seldom seen bumblebees (*Bombus terrestris*, $n > 20$) adopting suction methods, even at very low sugar concentrations (10%). The bumblebee tongue is similar but longer than the honey bee's one (about 4.5–8.5 mm).[21] Keeping all other parameters constant in eqn (18), except for setting a longer tongue immersed length $LI = 2.5$ mm and a suction region length $L = (4–8)$ mm, the critical viscosity for bumblebee becomes very low, $\mu^* < 0.001$ Pa s, *i.e.* below pure water viscosity. The suction regime is thus clearly out-of-range and is not used by *Bombus*. So, this model may explain why suction is only observed in some species. We also note that, physical mechanism is only one part of the fluid capture problem in animals, ethology should be another facet.

Feeding capability might reflect the health status of both pollinators and pollination.[22] This combined experimental and theoretical work builds a framework to evaluate the behavioral and physical dichotomy in feeding modes of bees, and provides the first quantification on the potential trade-off of the physics- or ethology-dominated feeding strategy. Tracking the delicate variation in feeding strategy selection may offer clues regarding the health of pollinators, even the deterioration in pollinations that accompany the ascending environmental stress.[23]

Conclusion

In summary, we observed honey bees using their proboscises to suck liquid and characterized the liquid flow during the sucking process. We proposed a physical model to describe the liquid and energy intake rates of honey bees' sucking method, which is in good agreement with the experimental data. We showed, that sucking is a more efficient way for transporting less viscous liquid through their complex proboscis structure, whereas lapping is more efficient for capturing more concentrated nectar. Notably, the models predict a critical viscosity, μ^*, which provide a nice rationale for the honey bee's sucking and lapping trade-off. The complex mouthpart structures and the switching of feeding methods featured in honey bees may not only offer insights into the coevolution between pollinators and flowering plants, but further inspire highly-adaptive microfluidics devices in the future.

Author contributions

J. Wei, J. Wu conducted the experiments and performed the visualization. F. Brau, P. Damman, A. Draux, HAB. Hua and J. Wei discussed and derived the physical modeling. Z. Wu supervised the project. J. Wei, J. Wu and Z. Wu drafted the original manuscript. F. Brau, P. Damman, A. Draux and HAB. Hua reviewed and revised the manuscript.

Conflicts of interest

There are no conflicts to declare.

Acknowledgements

References

1 L. A. Nilsson, *Nature*, 1988, **334**, 147–149.
2 C. Descamps, M. Quinet and A.-L. Jacquemart, *Environ. Exp. Bot.*, 2021, **182**, 104297.
3 S. W. Nicolson, *Nectaries Nectar*, 2007, 289–342.
4 G. Peralta, D. P. Vázquez, N. P. Chacoff, S. B. Lomáscolo, G. L. W. Perry and J. M. Tylianakis, *Ecol. Lett.*, 2020, **23**, 1107–1116.
5 D. W. Roubik and S. L. Buchmann, *Oecologia*, 1984, **61**, 1–10.
6 G. H. Pyke and N. M. Waser, *Biotropica*, 1981, **13**, 260–270.
7 W. Kim, T. Gilet and J. W. M. Bush, *Proc. Natl. Acad. Sci. U. S. A.*, 2011, **108**, 16618–16621.
8 W. Kim and J. W. M. Bush, *J. Fluid Mech.*, 2012, **705**, 7–25.
9 A. Lechantre, A. Draux, H. A. B. Hua, D. Michez, P. Damman and F. Brau, *Proc. Natl. Acad. Sci. U. S. A.*, 2021, **118**, 1–7.
10 C. Liao, Y. Xu, Y. Sun, M. S. Lehnert, W. Xiang, J. Wu and Z. Wu, *J. Insect Physiol.*, 2020, **124**, 104059.
11 J. Wei, Z. Huo, S. N. Gorb, A. Rico-Guevara, Z. Wu and J. Wu, *Biol. Lett.*, 2020, **16**, 1–5.
12 K. G. Kornev, A. A. Salamatin, P. H. Adler and C. E. Beard, *Sci. Rep.*, 2017, **7**, 1–18.
13 L. Courbin, E. Denieul, E. Dressaire, M. Roper, A. Ajdari and H. A. Stone, *Nat. Mater.*, 2007, **6**, 661–664.
14 A. Nasto, P. T. Brun and A. E. Hosoi, *Phys. Rev. Fluids*, 2018, **3**, 024002.
15 C. S. Jog, *Fluid Mechanics: Foundations and Applications of Mechanics*, Cambridge University Press, Cambridge, 3rd edn, 2015.
16 S. Kyritsi-Yiallourou and G. C. Georgiou, *Eur. J. Mech. – B Fluids*, 2018, **72**, 87–102.
17 K. A. Pivnick and J. N. McNeil, *Oecologia*, 1985, **66**, 226–237.
18 H. Yang, J. Wu and S. Yan, *Appl. Phys. Lett.*, 2014, **104**, 1–5.
19 V. Aroulmoji, V. Aguié-béghin, M. Mathlouthi and R. Douillard, *J. Colloid Interface Sci.*, 2004, **276**, 269–276.
20 L. D. Harder, *Development*, 1986, **i**, 309–315.
21 L. D. Harder, *Can. J. Zool.*, 1982, **60**, 1073–1079.
22 C. J. van der Kooi, M. Vallejo-Marín and S. D. Leonhardt, *Curr. Biol.*, 2021, **31**, R91–R99.
23 Adam J. Vanbergen, *Nature*, 2021, **596**, 351–352.